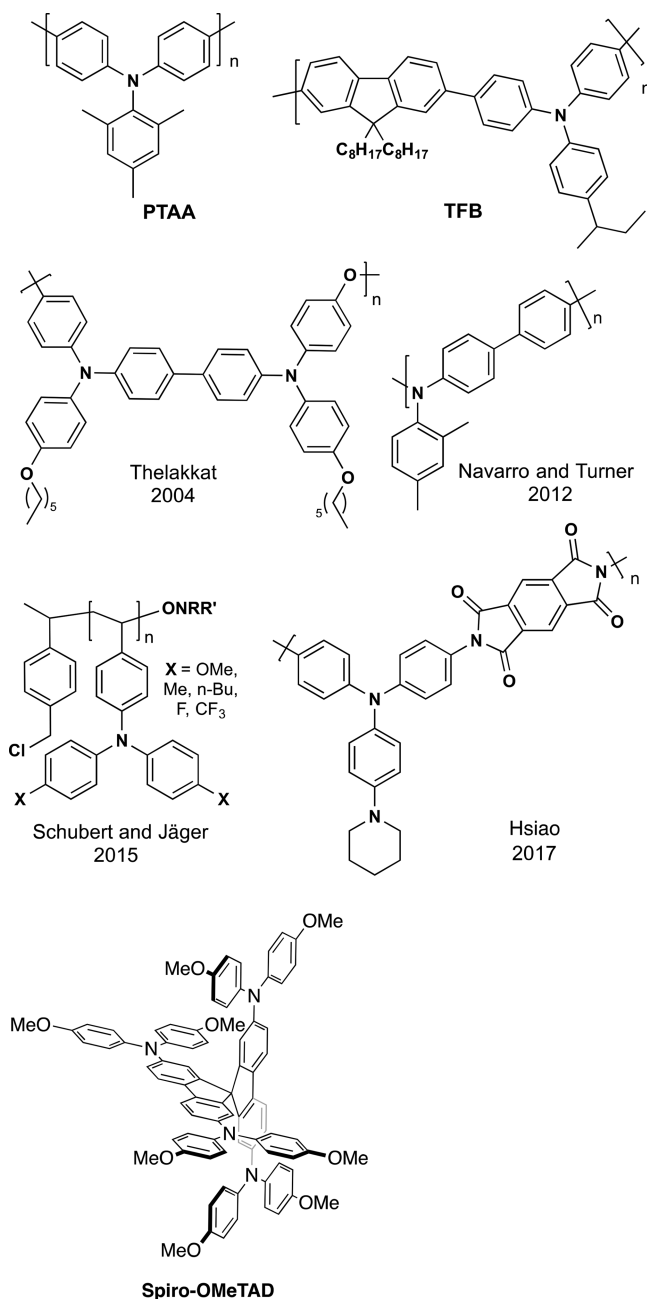


(PTAA) and poly(9,9-dioctylfluorene-*co*-*N*-(4-butylphenyl)-diphenylamine) (TFB; Chart 1), triarylamines have been

Chart 1. Representative Triarylamine-Containing Polymers and Molecular Spiro-OMeTAD



incorporated in the backbone or introduced as steric substituents.^{28–34} To date, PSC devices built with triarylamine-based hole transport polymers have lower power conversion efficiencies than those employing molecular Spiro-OMeTAD (>20% power conversion efficiency), spurring continued interest in viable polymeric alternatives.^{27,35–37}

The modular properties of polyketones make them compelling candidates for polytriarylamine-based (pTAA) hole transport polymers. A major challenge in hole transport material (HTM) design is finding routes to rationally maximize the extent of pore filling in device assembly.^{38,39} Good pore-filling and a stable amorphous state are desirable features for

HTMs,^{29,39} and high T_g is desirable to prevent microcrystalline states from forming in the HTM.³⁹ We hypothesized that a tacky aliphatic polyketone that has been functionalized with redox-relevant side chains may allow for independent control of pore filling and HOMO level—key to developing a rational HTM design scheme.⁴⁰

While pTAAs are widespread throughout optoelectronic research (Chart 1), most polymer designs require laborious syntheses of specialized monomers. Herein, we instead introduce redox-active pendants postpolymerization. Building upon prior methods^{13,17} we present a synthetic strategy for transforming a 1,4-polyketone into a library of functionalized polymers (Scheme 1B). A facile Sc(OTf)₃-catalyzed Paal–Knorr cyclization of poly(1-hexene-*alt*-CO) with aromatic amines allows for introduction of triarylamine pendants, azobenzenes, and other aromatic functionality. The incorporated groups yield polymers with specialized properties; azobenzene-derived polyketones are markedly more resistant to UV degradation than unfunctionalized polymers and undergo facile photoisomerization, while polyketones bearing triarylamine pendants form stable radical cations.

RESULTS AND DISCUSSION

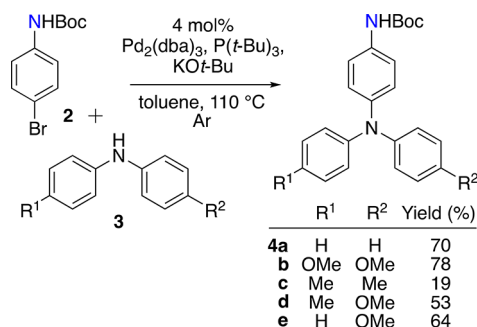
Polymerization Optimization. While typical polyketones are composed of ethylene or propylene comonomers, we chose the less common^{41,42} 1-hexene-derived polymer **1** (Scheme 1B) to maintain maximum organic solubility in successive functionalization reactions. Depending on catalyst, preparations of poly(1-hexene-*alt*-CO) can yield mixtures of interconvertible polyketone and polyspiroketal.^{43,44} [Pd(dppp)(MeCN)₂](BF₄)₂^{1,44–46} was used to ensure generation of an exclusively alternating polyketone structure.⁴⁷ The structure of polymer **1** was confirmed using ¹H NMR (methylene protons, 3.25–2.75 ppm in CDCl₃), ¹³C NMR (carbonyl carbons, 212 ppm), ATR-FTIR (carbonyl ν_{CO} , 1704 cm⁻¹), and GPC (molecular weights of the copolymer averaged $M_n = 2.2 \times 10^4$ and $M_w = 3.7 \times 10^4$ with dispersity of 1.6).

Postpolymerization Functionalization. The presence of regularly spaced carbonyls allows the polyketone to be functionalized with an amine via Paal–Knorr condensation.⁶ Catalysts can be used to promote mild (room temperature) Paal–Knorr reactions.^{13,14} Montmorillonite clay, iodine, iron phosphate, microwaves, and various Lewis acids have all previously been used as catalysts or promoters for small-molecule Paal–Knorr condensations.^{48–50} But even with a catalyst, polymer-based reactions are expected to be more challenging than molecular counterparts. Long polymer chains undergo cyclization at random places along the polymer backbone, leaving randomly spaced ketones trapped between the pyrroles. 86% conversion of the 1,4-diketone moieties to pyrroles is the statistical maximum.^{13,51}

Reaction of aniline with **1** achieves 27% conversion compared to the 60% previously reported with poly(ethylene-*alt*-CO).¹³ Since Sen found amine reactivity to depend on steric bulk, we first attempted a condensation of halogenated anilines and polyketone using a Paal–Knorr⁵⁰ condensation, followed by a Buchwald–Hartwig amination of resulting *N*-(haloaryl)pyrrole units with functionalized anilines. The latter reaction failed using *p*-toluidine or 2-pyrrolidinone, and so an alternative path was chosen where functionalized amines are used directly in Paal–Knorr cyclizations. Buchwald–Hartwig amination was used to join Boc-protected

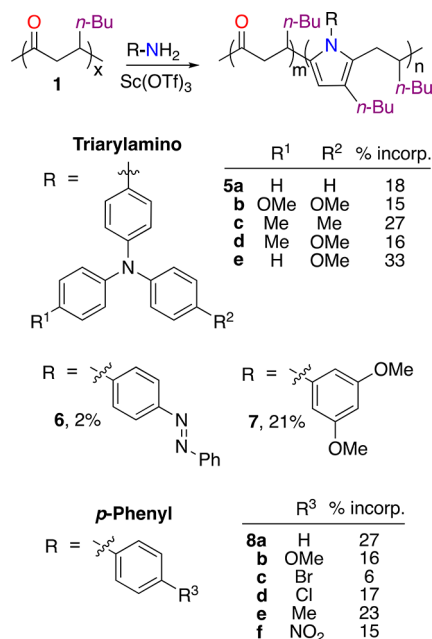
4-bromoaniline **2** and commercially available diarylamines **3a–e** to form amines **4a–e**, targeted for their steric bulk and inherent radical stability (Scheme 2). **4a–e** were then deprotected with 30% HCl and were stored as hydrochloride salts and neutralized as needed.

Scheme 2. Preparation of 4-Aminotriarylamines 4a–e for Polyketone Functionalization



Subsequent reaction of **4a–e** with **1** forms triarylamine-derived polymers **5a–e** (Chart 2). Similar reactions of

Chart 2. Functionalized Polymers Prepared via Paal–Knorr Reactions with 1^a



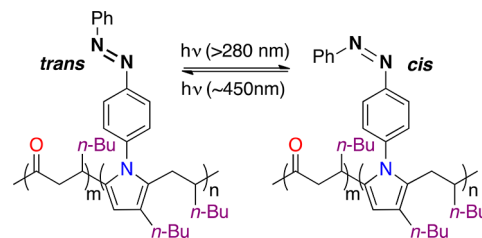
^aPercent incorporation is calculated from ¹H NMR spectra, integrating pyrrole ¹H resonances relative to an internal standard. See the Supporting Information for details.

functionalized anilines with **1** yield azobenzene-derived **6**, dimethoxyphenyl **7**, and para-substituted phenyl **8**. A typical reaction with an amine and the polyketone consisted of addition of 0.5 equiv of amine—chosen based on the reaction stoichiometry of two carbonyls per one amine—to a solution of polyketone in methylene chloride followed by addition of Sc(OTf)₃ (5 mol %). The reaction was heated to 40 °C for 24 h. When the reaction was halted, catalyst solids were removed via filtration and solvents removed under vacuum to yield the crude polymer. Purification of the pyrrole-functionalized

polymers was achieved by repeated precipitation from methylene chloride with methanol. The NMR assay used to ascertain the percent incorporation of functionalized units is described in the Supporting Information. No obvious correlation between percent incorporation and amine properties (sterics and electronics) is clear from the data collected.

Functionalized Polymer Properties. Azobenzene-Derived 6. Covalently incorporating azobenzene functionality postpolymerization can introduce photodegradation resistance, birefringence, and nonlinear optical effects^{52–56} while avoiding the expense of producing azobenzene-derived monomers.^{53,57,58} Nozaki and co-workers had previously prepared a similar polyketone with copolymerization of a 4-(5-hexenyloxy)azobenzene.⁵³ Nozaki did not comment on the appearance of the material. Here, the high molar extinction coefficient of azobenzene-functionalized **6** resulted in a brightly colored orange polymer despite relatively low percent incorporation (2%). Since the photoisomerization of azobenzene is known,⁵⁹ we studied the optical activity of **6** to observe a reversible *trans* → *cis* isomerization via irradiation with UV and visible light (Scheme 3). Azo π–π* and azo n–π* excitations trigger *trans* → *cis* and *cis* → *trans* isomerizations, respectively.⁵³

Scheme 3. Reversible Photoisomerization of Azobenzene Pendants of Polymer 6



To induce photoisomerization, **6** was dissolved in ethyl acetate and irradiated for 60 min with a medium pressure mercury lamp (400 W; 280–600 nm with a Pyrex filter). The polymer π–π* absorption band⁵² (ca. 338 nm) decreases after 60 min of irradiation, indicating conversion to the *cis* isomer (Figure 1A).^{52,58,60} Irradiating this sample subsequently with visible light (5.88 W blue LED, 440–460 nm) promoted the *cis*–*trans* isomerization (dashed, green trace), with a partial recovery of the π–π* *trans* absorption band. UV degradation was also assessed by measuring the change in polymer molecular weight after a period of irradiation (Figure 1B,C). Based on gel permeation chromatography (GPC) analysis, a sample of **1** irradiated by a 400 W mercury lamp rapidly decomposes, reaching a 33% reduction in molecular weight within 1 h. By comparison, the molecular weight of **6** is essentially unchanged after 1 h of irradiation, with a more gradual decomposition thereafter (Figure 1B,C), consistent with prior findings where azobenzene chromophores are added to polymers to prevent UV degradation.⁶⁰ Covalently linking the azo moiety to the polymer scaffold offers greater polymer stability and maximum photoresponsiveness of the azobenzene chromophore.⁶⁰

Triarylamine-Functionalized Polymers 5a–e. Triarylamines are common components of photovoltaic devices⁶¹ and OLEDs⁶² because of their facile oxidation, stability, and low crystallinity. In our hands, triarylamine-derived polymers **5a–e** all form stable radical cations upon oxidation with AgSbF₆.

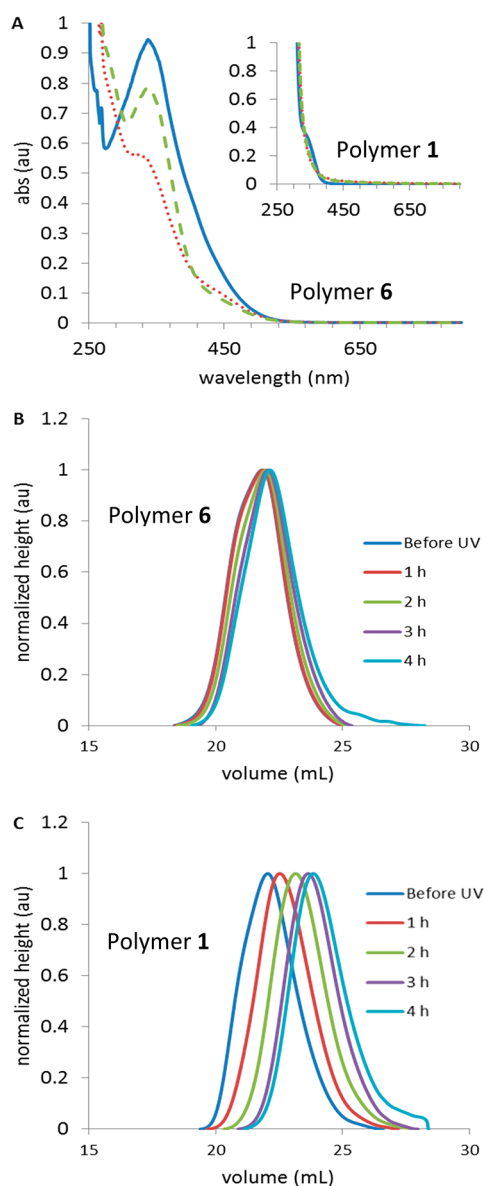


Figure 1. UV-vis spectrum of (A) azobenzene polymer 6 before UV exposure (solid blue trace), post-UV irradiation (dotted red trace), and post-visible irradiation (dashed green trace). Polyketone 1 before and after UV radiation is shown in the inset. GPC chromatograms of 6 (B) and 1 (C) during UV irradiation.

Before oxidation, the polymers resemble the other amine-functionalized polymers (dark brown, glassy solids). The UV-vis spectra obtained from dilute solutions of 5a–e had absorption maxima in the UV (250–350 nm) similar to other pTAAs and are assignable to π - π^* transitions from the triarylamine pendants (Figure 2).^{31–33} To oxidize the polymers, 2 mL of AgSbF_6 in methylene chloride (26 mM) was added dropwise to dilute solutions of each polymer ($\sim 0.01\%$ w/v in DCM). Each polymer solution initially became dark yellow; within a few minutes each developed its own color (a, tan/yellow; b, yellow-gray; c, tan/yellow; d, blue-gray; e, teal). All of the oxidized triarylmines absorbed at ~ 466 nm, and polymers bearing $-\text{OMe}$ groups (5b, 5d, 5e) showed additional absorptions at wavelengths >650 nm.

Electrochemical studies were conducted to complement the findings from chemical oxidation. Solution-phase cyclic

voltammetry (CV) and differential pulse voltammetry (DPV) have both been used previously to investigate electrochemical behavior of polymers bearing triarylmines.^{63–70} Here we relied on the more sensitive DPV to study the oxidation features of 1 and 5a–e (Figure 3). Changes in current (ΔI) for a given polymer indicate the relative amount of charge transferred, but a quantitative comparison of polymer electroactivities is complicated by effective triarylamine concentration; for a given polymer mass, a higher percent incorporation of a triarylamine will result in a higher absolute ΔI value. Each functionalized polymer 5a–e have distinct electrochemical signatures absent in the parent polyketone 1 between 0.5 and 1.2 V (vs Ag/AgCl). Electrochemical behavior of the triarylamine-functionalized polyketones depends upon the structure of the polymer's pendant group, indicating the oxidations are occurring at or around the triarylamine moieties. In addition, the oxidation features of the triarylamine polymers are similar to the behavior of molecular model compounds (vide infra).

Voltammetric features of polymers 5a–e resemble oxidation behavior of other triarylmines. For example, the strong influence of pendant functional groups upon oxidation potentials is consistent with profiles for other polymeric triarylmines (pTAAs).^{68,71–75} Oxidation of the pTAA nitrogen centers typically occurs 0.6–1.2 V vs Ag/AgCl, depending on aryl substituent. Monomeric triphenylamine itself undergoes oxidation at ca. 1.0 V⁷⁶ (vs Ag/AgCl unless otherwise noted), and polymers incorporating a *N,N*-diphenylamino substituent show oxidations between 0.8 and 1.1 V.^{76,77} The features of 5a and 5e voltammograms just above 1.0 V are therefore consistent with N-centered triarylamine oxidation. Methyl-substituted pTAAs oxidize at slightly lower potentials (ca. 0.8 V^{74,75}); similarly, methyl-substituted 5c and 5d show oxidations at ca. 0.85 V. One of the two features of 5b between 0.6 and 0.9 V could be N-centered triarylamine oxidation; methoxy-substituted pTAAs oxidize at ca. 0.65 V.⁷⁵

Additional oxidation features of polymers 5a–e are apparent, suggesting more complex behavior than found in other molecular and polymeric triarylmines. In the case of unsubstituted or *p*-methyl-substituted pTAAs, oxidation can induce intra- and intermolecular coupling between the aryl rings, forming carbazole units or dimers, which themselves can be oxidized.⁷² For *intermolecular* coupling, this can cause cross-linking of polymer chains and precipitation of the polymer, but in our hands, no solubility changes are observed upon oxidation. While the functionalization of 5b is random and limited to $\sim 15\%$ incorporation, a fraction of pendants could be close enough to one another to influence oxidation behavior, either as neighbors along a single polyketone chain or via through-space interactions between polymer chains. The additional oxidation features of 5a, 5b, and 5e (ca. 0.5 V) could be a result of chromophore stacking, which reduces oxidation potentials for aromatic polymers and DNA sequences.^{66,71,78–82} It has been shown previously that π stacking has a marked influence on lowering oxidation potentials of thiophene oligomers,⁸³ poly(dibenzofulvene)s,^{66,71,78} and similar pTAAs.⁶⁸ Therefore, precise redox potentials would be influenced by π stacking of the triarylamine residues of our materials.^{66,83,84} This phenomenon is evidenced when single molecules are contrasted against the polymeric forms (vide infra). We note that pyrrole oxidation is possible and may further complicate electrochemical behavior. An oxidizing environment could form radical cations centered

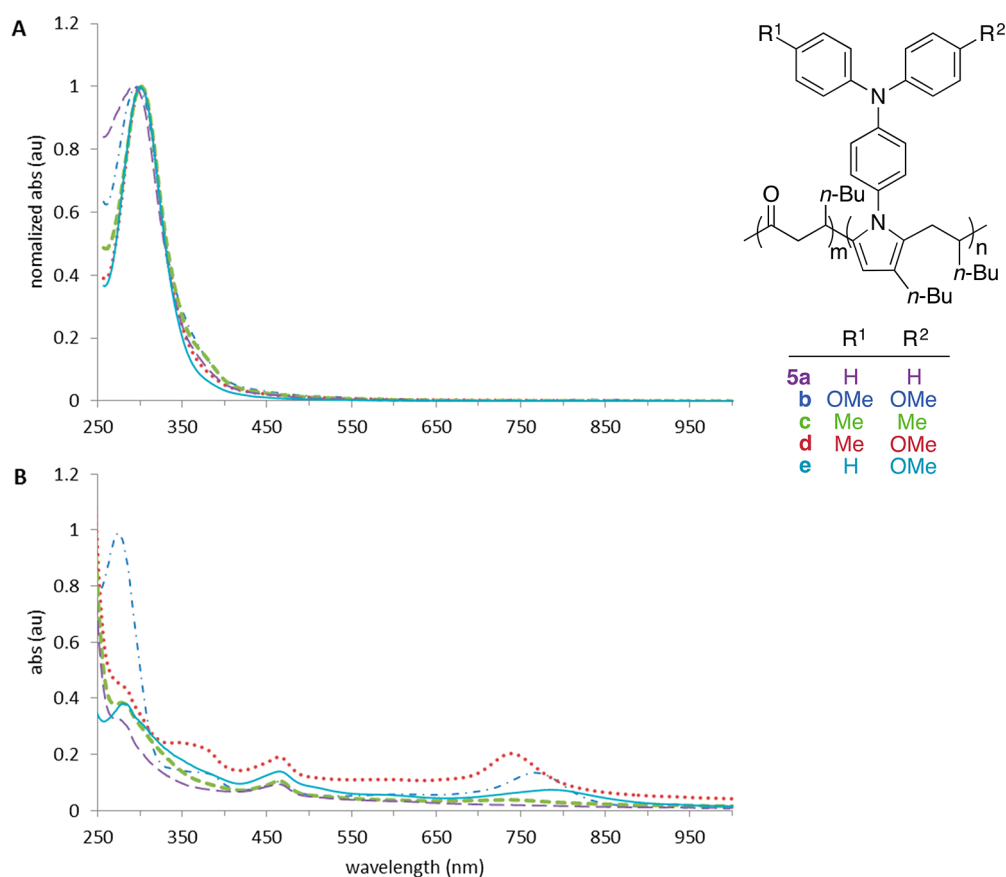


Figure 2. UV-vis spectra for polymers **5a–e** (A) prior to and (B) after reaction with AgSbF_6 in dichloromethane: **5a**, purple, dashed; **5b**, blue, dash-dot; **5c**, green, square dot; **5d**, red, round dot; **5e**, blue, solid.

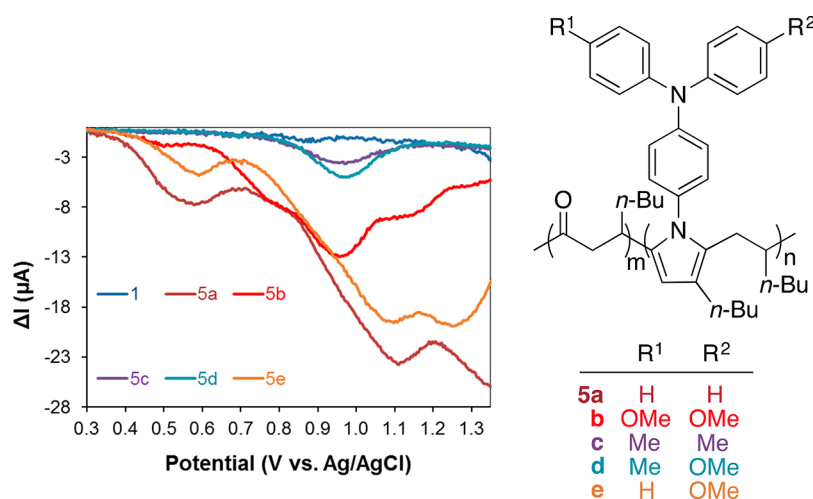


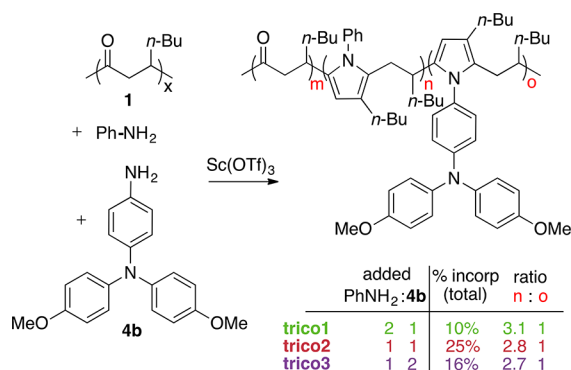
Figure 3. Differential pulse voltammograms for parent polyketone **1** and triarylamine-functionalized **5a–e**.

at the pyrrole rings, which could couple to oxidized triarylamine pendants within the same *N*-arylpyrrole unit or to radical cations nearby.⁷⁰ Cai et al.⁷⁷ propose complex oxidation behavior at *N*-(triarylmino)pyrrole units because of oxidations at both the pyrrole and triarylamine centers.

To further deconvolute the voltammogram of **5b**, we prepared mixed polymers from **1**, aniline, and the deprotected **4b** aniline, resulting in a random tricopolymers **trico1**, **trico2**, and **trico3** (Scheme 4). Despite varying the stoichiometry of aniline and triarylmino aniline, the previously optimized

conditions consistently provided an approximate 3:1 phenyl to triarylamine ratio. The overall percent incorporation (the amount of 1,4-diketones converted to an *N*-arylpyrrole) ranged from 10 to 25%, allowing for a comparison of overall triarylamine incorporation into the polymer. With increased percent incorporation of the triarylamine unit, there is an increase in ΔI of the shoulder at 0.75 V. This feature may reflect a localized decrease in oxidation potential due to proximity effects between triarylmines. Figure 4 compares the voltammograms of **trico1–3** and **5b** with the *N*-phenylpyrrole-

Scheme 4. A Random Tricopolymer from Condensation of 1, Aniline, and 4b^a



^aThe relative amounts of amine added in the preparation of each tricopolymer had little influence on the actual ratio of pyrrole substitutions (n:o) but allowed for testing a range of percent incorporation of triarylamine.

functionalized poly(1-hexene-*alt*-CO) (**8a**). While triarylamine-containing polymers demonstrate a pronounced oxidation feature near 0.9 V (vs Ag/AgCl), **8a** exhibits a ΔI_{\max} at a higher potential (1.15 V). Since **8a** does not exhibit features 0.8–1.0 V, the pyrrole ring and ketone functional groups are not alone responsible for the oxidation features observed with triarylamine polymers. **8a** does show a minor feature at 0.5 V, similar to **5b**, and so this feature may be due to backbone or *N*-arylpyrrole oxidation.

Properties of Substituted Pyrrole Model Compounds.

To gain insight into the redox behavior of the triarylamine pendants of the functionalized polymers **5a–e**, we prepared molecular models **9a–e** of the redox-active *N*-arylpyrrolyl units and explored their oxidation behavior in the absence of the polyketone polymer scaffold. The oxidation effects could then be compared to polymers **5a–e** to understand the origins of oxidative features in DPV electrochemistry as well as the UV–vis behavior of the chemically oxidized polymers. The preparation of the model compounds was straightforward, accessed via coupling *N*-(*p*-bromophenyl)pyrrole with commercially available diarylamines to yield compounds **9a–e** in moderate to excellent yields (Scheme 5). Once prepared, **9a–e** were chemically oxidized with AgSbF₆. The oxidized polymers **5a–e** and the oxidized molecular analogues **9a–e** all absorb strongly at ~450 nm (Table 1). UV–vis spectra for polymers **5b**, **5d**, and **5e** and molecules **9b** and **9e** feature an additional absorption band at ~750 nm—an absorption observed in other –OMe-substituted triarylamines.³³ For oxidized materi-

Scheme 5. Preparation of Compounds 9a–e

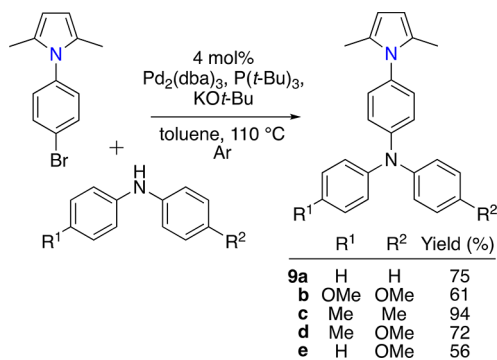


Table 1. Absorption Maxima for Functionalized Polymers and Molecular Model Compounds before (Neutral) and after (Oxidized) Treatment with AgSbF₆

	neutral (λ_{\max} , nm)		oxidized (λ_{\max} , nm)	
	polymers 5a–e	molecules 9a–e	polymers 5a–e	molecules 9a–e
diphenyl (5a , 9a)	293	303	463	445
dimethoxy (5b , 9b)	295	298	465, 767	445, 767
dimethyl (5c , 9c)	302	304	465	441
methoxymethyl (5d , 9d)	300	300	465, 739	470
methoxy (5e , 9e)	300	302	465, 785	448, 766

als, the triarylamine absorptions show negligible change upon immobilizing onto the polymer backbone. The substitution pattern and oxidized absorption maxima do not follow a clear trend. The –OMe-substituted materials were expected to be more red-shifted than the alkyl-substituted materials (red absorption wavelength in the order of dimethoxy > methoxymethyl > methoxy),^{33,85} but this relationship is not observed, perhaps due to the additional influence of the pyrrole moiety.

The electrochemical oxidation (DPV) features of the triarylamine model compounds differ from the corresponding polymer. As a representative example, the voltammograms for **5b** and **9b** (Figure 5) clearly indicate substantial changes in properties of triarylamine upon polymer incorporation. The more complex features of polymer **5b** (marked by an asterisk) are absent in molecule **9b**. One potential cause is poor oxidative stability of molecular pyrroles relative to moieties isolated in the polymer scaffolds.⁸⁶ Additionally, low concentrations of molecule **9b** do not permit interactions

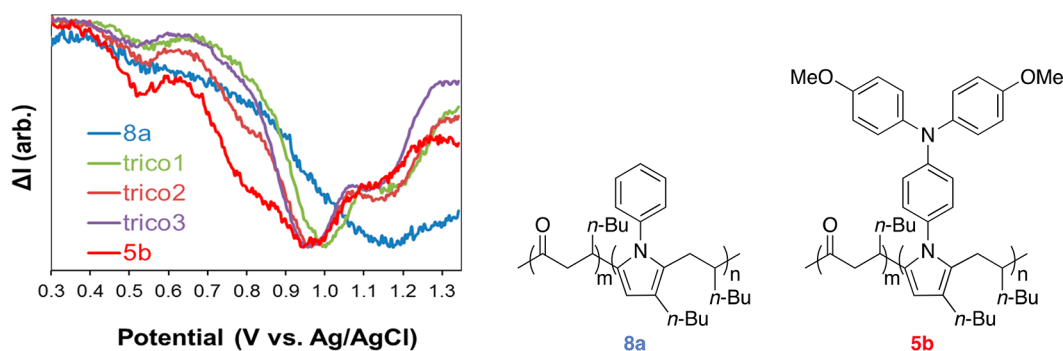


Figure 4. Differential pulse voltammograms for tricopolymers **trico1**, **trico2**, and **trico3** and polymers **8a** and **5b**.

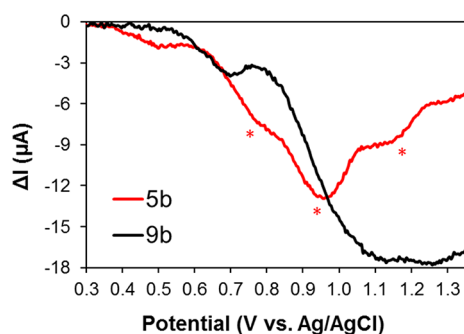


Figure 5. Voltammograms comparing the electrochemical behavior of **5b** and **9b** using DPV.

between triaryl amines, as we propose for the **5b** polymer (vide supra).

During our study of pyrrole-functionalized triaryl amines we have found that oxidation of the polymeric triaryl amines is more facile than molecular analogues. This is not unexpected; appending chromophores to polymer backbones is known to reduce the anodic potentials at which they oxidize.^{66,68,71,78,83} Previous studies have also reported a dependence on substitution pattern for the relative lifetimes of the formed radicals before intermolecular coupling reactions quench radical species.^{72,87} We, too, observe a dependence on substitution and oxidizing potential (see the [Supporting Information](#)). Oxidative events occurring between 0.25 and 0.75 V are reasonably assigned to the oxidation of the pyrrole ring itself⁸⁶ with the later features assigned to the oxidation of the triaryl amines. Pyrrole oxidation potentials are strongly dependent on substituent and factor strongly into the potentials required for pyrrole electropolymerization.⁸⁶

CONCLUSION

In this report we have prepared a polyketone from 1-hexene and carbon monoxide to functionalize postpolymerization. This investigation has led to a host of polymers with N-substituted pyrrolic functionality. With the synthesis of several aminotriaryl amines we were able to prepare polymers with triarylamine functionality (**5a–e**). These polymers' UV–vis spectra were drastically changed upon reaction with AgSbF₆, and their oxidized spectra support the formation of radical cationic species. Differential pulse voltammetry for each triarylamine polymer (**5a–e**) yielded a distinct electrochemical signature, confirming incorporation of optically and redox-active functionality into polyketone-based macromolecules. These observations are encouraging as they give potential to the search for redox-active polymers from readily accessible substrates with minimal synthetic effort. The modest incorporation of the arylamine pendants may require alternative routes to increase incorporation, however. We found that even a slight incorporation (2%) of azobenzene into the polyketone led to observable *trans* → *cis* photoisomerization for polymer **6** and significantly reduced photoinduced polymer decomposition. Further efforts in our laboratories will explore potential applications of functionalized polyketones.

EXPERIMENTAL SECTION

General Remarks. All reactions were performed in an inert atmosphere glovebox or using standard Schlenk techniques unless otherwise noted. NMR spectra are referenced to deuterated solvent

(e.g., CDCl₃ corrected to 7.26 ppm) or external standards (³¹P NMR, 85% phosphoric acid solution), and chemical shifts reported as ppm.

Apparatus. All NMR spectra were collected at room temperature on a Bruker 400 spectrometer (400 MHz) and a Bruker Avance 500 (500 MHz). Infrared spectra were collected as ATR-FTIR spectra using a Thermo Scientific Nicolet iS5 with a id5 ATR attachment. UV–vis spectra were collected using a Shimadzu UV-1800 double-beam spectrophotometer. Polymerizations were performed in a 100 mL Parr Instrument Co. 4590 microstirred reactor. GPC was performed with a Shimadzu LC 20-AT chromatograph using three PolarGel-M (300 × 7.5 mm²) columns and THF as an eluent. Calibration was done using standard PMMA samples (*M_p* range: 202–71800 Da). Solvents were purified by the Pure Process Technology purification system.

Electrochemical Measurements. Differential pulse voltammetry (DPV) measurements were performed using a 650E CH Instruments potentiostat. Polymers/molecular analogues of interest were dissolved in dichloromethane with 0.1 M tetrabutylammonium hexafluorophosphate (NBu₄PF₆) as a supporting electrolyte. Glassy carbon, silver wire, and platinum wire were used as a working, reference, and counter electrode, respectively. DPV was conducted by applying potential pulses of 50 mV amplitude for 50 ms duration over 500 ms period (potential waveform figure included in the [Supporting Information](#)).

Chemicals. Chemicals were used from Sigma-Aldrich Chemical Co., Oakwood Chemicals, Airgas, Kodak, and Tokyo Chemical Industry Co. without further purification with the exception of *p*-bromoaniline (Kodak) which was sublimed prior to use. Solvents used during air-free reactions were purified on a solvent purification system.

Preparation of [(Ph)₂P(CH₂)₃P(Ph)₂Pd(NCMe)₂](BF₄)₂.^{45,88} To a 100 mL flask [(NCMe)₄Pd](BF₄)₂⁸⁹ (0.533 g, 1.2 mmol), diphenylphosphinopropane (0.494 g, 1.2 mmol) and a magnetic stir bar were added. Acetonitrile (50 mL) was then added to the flask to produce a clear, bright yellow solution. The reaction was left to stir rapidly for 24 h. Once complete, the solvent was removed under vacuum to produce [(Ph)₂P(CH₂)₃P(Ph)₂Pd(NCMe)₂](BF₄)₂ as a bright yellow film (0.831 g, 89.3% yield). ¹H NMR (400 MHz, CDCl₃): δ 7.67 (dd, 7H), 7.49 (d, 3H), 2.93 (s, 4H), 2.30 (s, 2H), 1.90 (s, 6H). ³¹P NMR (202 MHz, CD₂Cl₂): δ 12.47.

Copolymerization of 1-Hexene and Carbon Monoxide (1). The procedure was adapted from Abu-Surrah et al.⁴² A pressure reactor was charged with [(Ph)₂P(CH₂)₃P(Ph)₂Pd(NCMe)₂](BF₄)₂ (0.1 mol %, 0.0457 g, 0.0595 mmol) followed by dichloromethane (10 mL), 1-hexene (7.43 mL, 59.5 mmol), and methanol (358 μL). The reactor was sealed and removed from the glovebox. The reactor was pressurized with carbon monoxide (1000 psi), and the reaction stirred at room temperature for 48 h. Once complete, the reaction solution was depressurized and quenched with an excess of methanol followed by removal of catalyst residues via silica gel plug. Solvent was removed under vacuum to yield the product as a translucent gel (2.05 g, 31% yield). ¹H NMR (500 MHz, CDCl₃): δ 3.09 (br), 2.90 (br), 2.65 (br), 2.57 (br), 2.38 (br), 2.36 (br), 1.61 (br), 1.25 (br), 0.88 (br).

***tert*-Butyl (4-Bromophenyl)carbamate (2).** Exclusion of air was not necessary. To a 250 mL round-bottom flask equipped with a stir bar freshly sublimed 4-bromoaniline (12.6 g, 73.1 mmol) was added followed by THF (80 mL). Once a homogeneous solution was formed, a solution of di-*tert*-butyl dicarbamate (17.7 g, 81.1 mmol) in THF (70 mL) was added dropwise via addition funnel over the course of 30 min. After addition was complete the addition funnel was exchanged for a condenser, and the reaction was refluxed for 24 h or until judged complete via TLC (1:10 ethyl acetate:hexanes). The product was then purified via flash chromatography to afford **3** as a white solid (4.18 g, 86.4% yield). ¹H NMR (500 MHz, CD₂Cl₂): δ 7.43–7.23 (m, 4H), 6.57 (s, 1H), 1.49 (s, 9H).

***N*-(4-Bromophenyl)-2,5-dimethylpyrrole.** Prepared via the work of Chen et al. without exclusion of air.⁵⁰ 2,5-Hexanedione (5 mmol), 4-bromoaniline (5 mmol), and Sc(OTf)₃ (0.05 mmol, 1 mol %) were added to a round-bottom flask equipped with a stir bar. The

reaction stirred at 30 °C for 30 min or until complete. After the required time a tan solid was collected via filtration and washed with cold water to yield an off-white solid (1.04 g, 67% yield). ¹H NMR (400 MHz, CD₂Cl₂): δ 7.60 (d, 2H), 7.09 (d, 2H), 5.83 (s, 2H), 2.00 (s, 6H).

General Cross-Coupling Procedure for Triarylaminines (4 and 9). To a Schlenk flask 3 (1.37 g, 5.03 mmol), diphenylamine (0.425 g, 2.52 mmol), tris(dibenzylideneacetone)dipalladium (0.184 g, 0.201 mmol, 4 mol %), tri(*tert*-butyl)phosphine (0.163 g, 0.805 mmol, 16 mol %), potassium *tert*-butoxide (1.13 g, 10.1 mmol), and toluene (15 mL) were added. The flask was removed from the glovebox and heated to 111 °C under nitrogen for 24 h or until judged complete by TLC. Once completed, the reaction was cooled to room temperature and extracted via aqueous work-up. The crude product was purified via flash chromatography (1:10 ethyl acetate:hexanes) and dried under vacuum to afford **4a** as an opalescent foam (0.624 g, 70% yield). ¹H NMR (500 MHz, CD₂Cl₂): δ 7.33–7.19 (m, 6H), 7.11–6.87 (m, 8H), 6.52 (s, 1H), 1.49 (s, 9H).

4-Aminotriphenylamine-HCl. **4a** (0.624 g, 1.73 mmol) was added to a round-bottom flask, and a premixed solution of 30% HCl in ethyl acetate (5 mL) is slowly added to dissolve the solid. Once homogeneous, the reaction was concentrated to induce precipitation. The solid was filtered and washed with water to afford a beige solid (0.342 g, 66.5% yield). ¹H NMR (500 MHz, (CD₃)₂SO): δ 9.67 (s, 3H), 7.35–7.27 (m, 4H), 7.22–7.15 (m, 2H), 7.10–6.97 (m, 8H).

Preparation of Pyrrole-Functionalized Polyketone (5a–e, 6, 7, and 8a–f). Exclusion of air was not necessary. To a solution of **1** (0.500 g, 4.46 mmol) in dichloromethane (10 mL) the 1° amine was added (4.46 mmol) followed by Sc(OTf)₃ (5 mol %, 0.223 mmol). The reaction was stirred at 40 °C for 24 h, after which time the reaction mixture was cooled to room temperature and filtered to remove the catalyst. The product was purified via repeated precipitation in methanol. If triarylaminines were used (**4a–e**), the triarylamine-HCl was extracted with base (2 M Na₂CO_{3(aq)}) prior to use.

Photoisomerization of Polyaminoazopyrrole (6). **6** was dissolved in ethyl acetate and sealed in a cuvette. The cuvette was affixed to the water jacket which was used to cool the lamp, and the solution was irradiated for 60 min with a medium pressure mercury lamp (400 W; 280–600 nm with a Pyrex filter) to induce photoisomerization. A UV–vis spectrum was collected immediately after irradiation. Irradiating the sample with visible light from a 5.88 W blue LED (440–460 nm; 447.5 λ_{max}) for 60 min induced the *cis* → *trans* isomerization; the UV–vis spectrum was collected immediately after irradiation. More information about the LED assembly can be found in the [Supporting Information](#).

■ ASSOCIATED CONTENT

📄 Supporting Information

The Supporting Information is available free of charge on the ACS Publications website at DOI: [10.1021/acs.macromol.8b01629](https://doi.org/10.1021/acs.macromol.8b01629).

¹H NMR spectra of starting materials, catalyst, and polymer; calculation of percent conversion of polymer functionalization; UV–vis spectra of **9a–e** before and after AgSbF₆ oxidation (PDF)

■ AUTHOR INFORMATION

Corresponding Author

*E-mail: dob@temple.edu.

ORCID

Katherine A. Willets: 0000-0002-1417-4656

Graham E. Dobereiner: 0000-0001-6885-2021

Notes

The authors declare no competing financial interest.

■ ACKNOWLEDGMENTS

Acknowledgment is made to the Donors of the American Chemical Society Petroleum Research Fund for partial support of this research. Support for the NMR facility at Temple University by a CURE grant from the Pennsylvania Department of Health is gratefully acknowledged. This work was supported by a Targeted Research Grant from the Temple University Office of the Vice Provost for Research. This material is based upon work supported by the U.S. Department of Energy, Office of Science, Office of Basic Energy Sciences under Award DE-SC0010307. The authors acknowledge Eromon O. Asikhia for his synthetic contribution to this work and Dr. Brenden P. Derstine for experimental assistance.

■ REFERENCES

- (1) Sen, A. Mechanistic aspects of metal-catalyzed alternating copolymerization of olefins with carbon monoxide. *Acc. Chem. Res.* **1993**, *26* (6), 303–310.
- (2) Zehetmaier, P. C.; Vagin, S. I.; Rieger, B. Functionalization of aliphatic polyketones. *MRS Bull.* **2013**, *38* (03), 239–244.
- (3) Beller, M.; Steinhoff, B. A.; Zoeller, J. R.; Cole-Hamilton, D. J.; Drent, E.; Wu, X.; Neumann, H.; Ito, S.; Nozaki, K. In *Applied Homogeneous Catalysis with Organometallic Compounds*; Cornils, B., Herrmann, W. A., Beller, M., Paciello, R., Eds.; Wiley-VCH: Weinheim, 2017; pp 91–190.
- (4) Hamarneh, A. I.; Heeres, H. J.; Broekhuis, A. A.; Sjollem, K. A.; Zhang, Y.; Picchioni, F. Use of soy proteins in polyketone-based wood adhesives. *Int. J. Adhes. Adhes.* **2010**, *30* (7), 626–635.
- (5) Kinneberg, P. A.; Armer, T. A.; Van Breen, A. W.; Barton, R. E. C.; Klei, E. Polyketone-based structural adhesive. US 4880904, November 14, 1989.
- (6) Bianchini, C.; Meli, A. Alternating copolymerization of carbon monoxide and olefins by single-site metal catalysis. *Coord. Chem. Rev.* **2002**, *225* (1–2), 35–66.
- (7) Bartsch, G. C.; Malinova, V.; Volkmer, B. E.; Hautmann, R. E.; Rieger, B. CO-alkene polymers are biocompatible scaffolds for primary urothelial cells in vitro and in vivo. *BJU Int.* **2007**, *99* (2), 447–453.
- (8) Jiang, Z.; Sangneria, S.; Sen, A. Polymers Incorporating Backbone Thiophene, Furan, and Alcohol Functionalities Formed Through Chemical Modifications of Alternating Olefin-Carbon Monoxide Copolymers. *J. Polym. Sci., Part A: Polym. Chem.* **1994**, *32*, 841–847.
- (9) Cheng, C.; Guironnet, D.; Barborak, J.; Brookhart, M. Preparation and characterization of conjugated polymers made by postpolymerization reactions of alternating polyketones. *J. Am. Chem. Soc.* **2011**, *133* (25), 9658–61.
- (10) Green, M. J.; Lucy, A. R.; Lu, S.-Y.; Paton, R. M. Functionalisation of alkene-carbon monoxide alternating copolymers via transketalisation reactions. *J. Chem. Soc., Chem. Commun.* **1994**, *18*, 2063–2064.
- (11) Lu, S.-Y.; Paton, R. M.; Green, M. J.; Lucy, A. R. Synthesis and characterization of polyketoximes derived from alkene-carbon monoxide copolymers. *Eur. Polym. J.* **1996**, *32* (11), 1285–1288.
- (12) Sen, A.; Jiang, Z.; Chen, J. T. Novel nitrogen-containing heterocyclic polymers derived from the alternating ethylene-carbon monoxide copolymer. *Macromolecules* **1989**, *22* (4), 2012–2014.
- (13) Chen, J.-T.; Yeh, Y.-S.; Sen, A. Synthesis and characterization of N-substituted poly(ethylenepyrrole): functionalization of ethylene-carbon monoxide alternating copolymers. *J. Chem. Soc., Chem. Commun.* **1989**, *14*, 965–967.
- (14) Zhang, Y.; Broekhuis, A. A.; Stuart, M. C. A.; Picchioni, F. Polymeric amines by chemical modifications of alternating aliphatic polyketones. *J. Appl. Polym. Sci.* **2008**, *107* (1), 262–271.
- (15) Mul, W. P.; Dirkszwaiger, H.; Broekhuis, A. A.; Heeres, H. J.; van der Linden, A. J.; Guy Orpen, A. Highly active, recyclable catalyst for the manufacture of viscous, low molecular weight, CO–ethene–

propene-based polyketone, base component for a new class of resins. *Inorg. Chim. Acta* **2002**, *327* (1), 147–159.

(16) Kiovsky, T. E.; Kromer, R. C. Polymeric pyrrolic derivative. US 3979374A, June 13, 1975.

(17) Wong, P. K. Pyridine derivatives. US 5047501A, December 29, 1987.

(18) Wong, P. K. Polymeric polyketone derivatives. EP 0324998A2, December 29, 1987.

(19) Sinai-Zingde, G. D. Polymer formed by reaction of a polyketone and an amino acid. US 5605988A, March 16, 1992.

(20) Brown, S. L. Polymers and processes for their preparation. EP 0400903A2, May 31, 1989.

(21) Brown, S. L. Poly pyrrole from co/olefin terpolymer. US 5081207A, May 31, 1989.

(22) Broekhuis, A. A.; Freriks, J. Polymeric amines. US 5952459, March 24, 1997.

(23) Drent, E.; Budzelaar, P. H. M. Palladium-Catalyzed Alternating Copolymerization of Alkenes and Carbon Monoxide. *Chem. Rev.* **1996**, *96* (2), 663–682.

(24) Jiang, Z.; Sanganeria, S.; Sen, A. Polymers incorporating backbone thiophene, furan, and alcohol functionalities formed through chemical modifications of alternating olefin-carbon monoxide copolymers. *J. Polym. Sci., Part A: Polym. Chem.* **1994**, *32* (5), 841–847.

(25) Toncelli, C.; Haijer, A.; Alberts, F.; Broekhuis, A. A.; Picchioni, F. The Green Route from Carbon Monoxide Fixation to Functional Polyamines: A Class of High-Performing Metal Ion Scavengers. *Ind. Eng. Chem. Res.* **2015**, *54* (38), 9450–9457.

(26) Cheng, C.; Guironnet, D.; Barborak, J.; Brookhart, M. Preparation and Characterization of Conjugated Polymers Made by Postpolymerization Reactions of Alternating Polyketones. *J. Am. Chem. Soc.* **2011**, *133* (25), 9658–9661.

(27) Saliba, M.; Orlandi, S.; Matsui, T.; Aghazada, S.; Cavazzini, M.; Correa-Baena, J. P.; Gao, P.; Scopelliti, R.; Mosconi, E.; Dahmen, K. H.; De Angelis, F.; Abate, A.; Hagfeldt, A.; Pozzi, G.; Graetzel, M.; Nazeeruddin, M. K. A molecularly engineered hole-transporting material for efficient perovskite solar cells. *Nat. Energy* **2016**, *1*, 15017.

(28) Hsiao, S.-H.; Hsiao, Y.-H. Synthesis and electrochemical properties of new redox-active polyimides with (1-piperidinyl)-triphenylamine moieties. *High Perform. Polym.* **2017**, *29* (4), 431–440.

(29) Ishida, N.; Wakamiya, A.; Saeki, A. Quantifying Hole Transfer Yield from Perovskite to Polymer Layer: Statistical Correlation of Solar Cell Outputs with Kinetic and Energetic Properties. *ACS Photonics* **2016**, *3* (9), 1678–1688.

(30) Kisselev, R.; Thelakkat, M. Synthesis and Characterization of Poly(triarylamine)s Containing Isothianaphthene Moieties. *Macromolecules* **2004**, *37* (24), 8951–8958.

(31) Matsui, T.; Petrikyte, I.; Malinauskas, T.; Domanski, K.; Daskeviciene, M.; Steponaitis, M.; Gratia, P.; Tress, W.; Correa-Baena, J.-P.; Abate, A.; Hagfeldt, A.; Grätzel, M.; Nazeeruddin, M. K.; Getautis, V.; Saliba, M. Additive-Free Transparent Triarylamine-Based Polymeric Hole-Transport Materials for Stable Perovskite Solar Cells. *ChemSusChem* **2016**, *9* (18), 2567–2571.

(32) Schlotthauer, T.; Schroot, R.; Glover, S.; Hammarström, L.; Jäger, M.; Schubert, U. S. A multidonor-photosensitizer-multi-acceptor triad for long-lived directional charge separation. *Phys. Chem. Chem. Phys.* **2017**, *19* (42), 28572–28578.

(33) Schroot, R.; Schubert, U. S.; Jäger, M. Block Copolymers for Directional Charge Transfer: Synthesis, Characterization, and Electrochemical Properties of Redox-Active Triarylamines. *Macromolecules* **2015**, *48* (7), 1963–1971.

(34) Sprick, R. S.; Hoyos, M.; Navarro, O.; Turner, M. L. Synthesis of poly(triarylamine)s by C–N coupling catalyzed by (N-heterocyclic carbene)-palladium complexes. *React. Funct. Polym.* **2012**, *72* (5), 337–340.

(35) Guo, Y.; Liu, C.; Inoue, K.; Harano, K.; Tanaka, H.; Nakamura, E. Enhancement in the efficiency of an organic-inorganic hybrid solar

cell with a doped P3HT hole-transporting layer on a void-free perovskite active layer. *J. Mater. Chem. A* **2014**, *2* (34), 13827–13830.

(36) Ahn, N.; Son, D.-Y.; Jang, I.-H.; Kang, S. M.; Choi, M.; Park, N.-G. Highly Reproducible Perovskite Solar Cells with Average Efficiency of 18.3% and Best Efficiency of 19.7% Fabricated via Lewis Base Adduct of Lead(II) Iodide. *J. Am. Chem. Soc.* **2015**, *137* (27), 8696–8699.

(37) Huang, C.; Fu, W.; Li, C.-Z.; Zhang, Z.; Qiu, W.; Shi, M.; Heremans, P.; Jen, A. K. Y.; Chen, H. Dopant-Free Hole-Transporting Material with a C_{3h} Symmetrical Truxene Core for Highly Efficient Perovskite Solar Cells. *J. Am. Chem. Soc.* **2016**, *138* (8), 2528–2531.

(38) Melas-Kyriazi, J.; Ding, I. K.; Marchioro, A.; Punzi, A.; Hardin, B. E.; Burkhard, G. F.; Tétreault, N.; Grätzel, M.; Moser, J.-E.; McGehee, M. D. The Effect of Hole Transport Material Pore Filling on Photovoltaic Performance in Solid-State Dye-Sensitized Solar Cells. *Adv. Energy Mater.* **2011**, *1* (3), 407–414.

(39) Agarwala, P.; Kabra, D. A review on triphenylamine (TPA) based organic hole transport materials (HTMs) for dye sensitized solar cells (DSSCs) and perovskite solar cells (PSCs): evolution and molecular engineering. *J. Mater. Chem. A* **2017**, *5* (4), 1348–1373.

(40) Zhang, W.; Cheng, Y.; Yin, X.; Liu, B. Solid-State Dye-Sensitized Solar Cells with Conjugated Polymers as Hole-Transporting Materials. *Macromol. Chem. Phys.* **2011**, *212* (1), 15–23.

(41) Abu-Surrah, A. S.; Rieger, B. High molecular weight 1-olefin/carbon monoxide copolymers: a new class of versatile polymers. *Top. Catal.* **1999**, *7* (1–4), 165–177.

(42) Abu-Surrah, A. S.; Wursche, R.; Rieger, B. Polyketone materials: control of glass transition temperature and surface polarity by co- and terpolymerization of carbon monoxide with higher 1-olefins. *Macromol. Chem. Phys.* **1997**, *198* (4), 1197–1208.

(43) Nozaki, K.; Kawashima, Y.; Nakamoto, K.; Hiyama, T. Alternating Copolymerization of Various Alkenes with Carbon Monoxide Using a Cationic Pd(II) Complex of (R,S)-BINAPHOS as an Initiator. *Polym. J.* **1999**, *31* (11), 1057.

(44) Nozaki, K.; Hiyama, T. Stereoselective alternating copolymerization of carbon monoxide with alkenes. *J. Organomet. Chem.* **1999**, *576* (1), 248–253.

(45) Drent, E.; Budzelaar, P. H. M. Palladium-Catalyzed Alternating Copolymerization of Alkenes and Carbon Monoxide. *Chem. Rev.* **1996**, *96* (2), 663.

(46) Beckmann, U.; Eichberger, E.; Rufinska, A.; Sablong, R.; Klau, W. Nickel(II) catalyzed co-polymerisation of CO and ethene: Formation of polyketone vs. polyethylene – The role of co-catalysts. *J. Catal.* **2011**, *283* (2), 143–148.

(47) Pérez-Foullerat, D.; Meier, U. W.; Hild, S.; Rieger, B. High-Molecular-Weight Polyketones from Higher α -Olefins: A General Method. *Macromol. Chem. Phys.* **2004**, *205* (17), 2292–2302.

(48) Banik, B. K.; Samajdar, S.; Banik, I. Simple synthesis of substituted pyrroles. *J. Org. Chem.* **2004**, *69* (1), 213–6.

(49) Samadi, M.; Behbahani, F. K. The Application of Iron(III) Phosphate in the Synthesis of N-substituted Pyrroles. *Journal of the Chilean Chemical Society* **2015**, *60* (2), 2881–2884.

(50) Chen, J.; Wu, H.; Zheng, Z.; Jin, C.; Zhang, X.; Su, W. An approach to the Paal–Knorr pyrroles synthesis catalyzed by Sc(OTf)₃ under solvent-free conditions. *Tetrahedron Lett.* **2006**, *47* (30), 5383–5387.

(51) Flory, P. J. Intramolecular Reaction between Neighboring Substituents of Vinyl Polymers. *J. Am. Chem. Soc.* **1939**, *61* (6), 1518–1521.

(52) Bandara, H. M. D.; Burdette, S. C. Photoisomerization in different classes of azobenzene. *Chem. Soc. Rev.* **2012**, *41* (5), 1809–1825.

(53) Kosaka, N.; Oda, T.; Hiyama, T.; Nozaki, K. Synthesis and Photoisomerization of Optically Active 1,4-Polyketones Substituted by Azobenzene Side Chains. *Macromolecules* **2004**, *37* (9), 3159–3164.

(54) Natansohn, A.; Rochon, P. Photoinduced Motions in Azo-Containing Polymers. *Chem. Rev.* **2002**, *102* (11), 4139–4176.

- (55) Qiu, F.; Cao, Y.; Xu, H.; Jiang, Y.; Zhou, Y.; Liu, J. Synthesis and properties of polymer containing azo-dye chromophores for nonlinear optical applications. *Dyes Pigm.* **2007**, *75* (2), 454–459.
- (56) Wen, H.; Zhang, W.; Weng, Y.; Hu, Z. Photomechanical bending of linear azobenzene polymer. *RSC Adv.* **2014**, *4* (23), 11776–11781.
- (57) Qiu, F.; Cao, Y.; Xu, H.; Jiang, Y.; Zhou, Y.; Liu, J. Synthesis and properties of polymer containing azo-dye chromophores for nonlinear optical applications. *Dyes Pigm.* **2007**, *75* (2), 454–459.
- (58) Takenaka, Y.; Osakada, K.; Nakano, M.; Ikeda, T. A Liquid Crystalline Polyketone Prepared from Allene Having an Azobenzene Substituent and Carbon Monoxide. *Macromolecules* **2003**, *36* (4), 1414–1416.
- (59) Wang, X. Trans–Cis Isomerization. In *Azo Polymers*; Springer: Berlin, 2017; pp 19–56.
- (60) Yager, K. G.; Barrett, C. J. Azobenzene Polymers for Photonic Applications. In *Smart Light-Responsive Materials*; John Wiley & Sons, Inc.: 2008.
- (61) Wang, J.; Liu, K.; Ma, L.; Zhan, X. Triarylamine: Versatile Platform for Organic, Dye-Sensitized, and Perovskite Solar Cells. *Chem. Rev.* **2016**, *116* (23), 14675–14725.
- (62) Shirota, Y.; Kageyama, H. Charge Carrier Transporting Molecular Materials and Their Applications in Devices. *Chem. Rev.* **2007**, *107* (4), 953–1010.
- (63) Huang, C.; Potscavage, W. J.; Tiwari, S. P.; Sutcu, S.; Barlow, S.; Kippelen, B.; Marder, S. R. Polynorbornenes with pendant perylene diimides for organic electronic applications. *Polym. Chem.* **2012**, *3* (10), 2996–3006.
- (64) Inagi, S.; Kaihatsu, N.; Hayashi, S.; Fuchigami, T. Facile synthesis of a variety of triarylamine-based conjugated polymers and tuning of their optoelectronic properties. *Synth. Met.* **2014**, *187*, 81–85.
- (65) Behl, M.; Hattemer, E.; Brehmer, M.; Zentel, R. Tailored Semiconducting Polymers: Living Radical Polymerization and NLO-Functionalization of Triphenylamines. *Macromol. Chem. Phys.* **2002**, *203* (3), 503–510.
- (66) Nakano, T.; Yade, T. Synthesis, Structure, and Photophysical and Electrochemical Properties of a π -Stacked Polymer. *J. Am. Chem. Soc.* **2003**, *125* (50), 15474–15484.
- (67) Page, Z. A.; Chiu, C.-Y.; Narupai, B.; Laitar, D. S.; Mukhopadhyay, S.; Sokolov, A.; Hudson, Z. M.; Bou Zerdan, R.; McGrath, A. J.; Kramer, J. W.; Barton, B. E.; Hawker, C. J. Highly Photoluminescent Nonconjugated Polymers for Single-Layer Light Emitting Diodes. *ACS Photonics* **2017**, *4* (3), 631–641.
- (68) Wang, H.; Wang, Y.; Ye, X.; Hayama, H.; Sugino, H.; Nakano, H.; Nakano, T. Stacked poly(vinyl ketone)s with accumulated push-pull triphenylamine moieties in the side chain. *Polym. Chem.* **2017**, *8* (4), 708–714.
- (69) Sauve, E. R.; Tonge, C. M.; Paisley, N. R.; Cheng, S.; Hudson, Z. M. Cu(0)-RDRP of acrylates based on p-type organic semiconductors. *Polym. Chem.* **2018**, *9* (12), 1397–1403.
- (70) Pittelli, S. L.; Shen, D. E.; Österholm, A. M.; Reynolds, J. R. Chemical Oxidation of Polymer Electrodes for Redox Active Devices: Stabilization through Interfacial Interactions. *ACS Appl. Mater. Interfaces* **2018**, *10* (1), 970–978.
- (71) Luo, J.; Wang, Y.; Nakano, T. Free-Radical Copolymerization of Dibenzofulvene with (Meth)acrylates Leading to π -Stacked Copolymers. *Polymers* **2018**, *10* (6), 654.
- (72) Yurchenko, O.; Heinze, J.; Ludwigs, S. Electrochemically Induced Formation of Independent Conductivity Regimes in Polymeric Triphenylbenzidine Systems. *ChemPhysChem* **2010**, *11* (8), 1637–1640.
- (73) Hsiao, S.-H.; Liou, G.-S.; Kung, Y.-C.; Hsiung, T.-J. Synthesis and properties of new aromatic polyamides with redox-active 2,4-dimethoxytriphenylamine moieties. *J. Polym. Sci., Part A: Polym. Chem.* **2010**, *48* (15), 3392–3401.
- (74) Choi, K.; Yoo, S. J.; Sung, Y.-E.; Zentel, R. High Contrast Ratio and Rapid Switching Organic Polymeric Electrochromic Thin Films Based on Triarylamine Derivatives from Layer-by-Layer Assembly. *Chem. Mater.* **2006**, *18* (25), 5823–5825.
- (75) Bender, T. P.; Graham, J. F.; Duff, J. M. Effect of Substitution on the Electrochemical and Xerographic Properties of Triarylamines: Correlation to the Hammett Parameter of the Substituent and Calculated HOMO Energy Level. *Chem. Mater.* **2001**, *13* (11), 4105–4111.
- (76) Thelakkat, M. Star-Shaped, Dendrimeric and Polymeric Triarylamines as Photoconductors and Hole Transport Materials for Electro-Optical Applications. *Macromol. Mater. Eng.* **2002**, *287* (7), 442–461.
- (77) Cai, S.; Wang, S.; Wei, D.; Niu, H.; Wang, W.; Bai, X. Multifunctional polyamides containing pyrrole unit with different triarylamine units owning electrochromic, electrofluorochromic and photoelectron conversion properties. *J. Electroanal. Chem.* **2018**, *812*, 132–142.
- (78) Nageh, H.; Wang, Y.; Nakano, T. Cationic polymerization of dibenzofulvene leading to a π -stacked polymer. *Polymer* **2018**, *144*, 51–56.
- (79) Merlani, M.; Koyama, Y.; Sato, H.; Geng, L.; Barbakadze, V.; Chankvetadze, B.; Nakano, T. Ring-opening polymerization of a 2,3-disubstituted oxirane leading to a polyether having a carbonyl–aromatic π -stacked structure. *Polym. Chem.* **2015**, *6* (11), 1932–1936.
- (80) Gudeangadi, P. G.; Sakamoto, T.; Shichibu, Y.; Konishi, K.; Nakano, T. Chiral Polyurethane Synthesis Leading to π -Stacked 2/1-Helical Polymer and Cyclic Compounds. *ACS Macro Lett.* **2015**, *4* (9), 901–906.
- (81) Rhodes, W. Hypochromism and Other Spectral Properties of Helical Polynucleotides. *J. Am. Chem. Soc.* **1961**, *83* (17), 3609–3617.
- (82) Tinoco, I. Hypochromism in Polynucleotides I. *J. Am. Chem. Soc.* **1960**, *82* (18), 4785–4790.
- (83) Knoblock, K. M.; Silvestri, C. J.; Collard, D. M. Stacked Conjugated Oligomers as Molecular Models to Examine Interchain Interactions in Conjugated Materials. *J. Am. Chem. Soc.* **2006**, *128* (42), 13680–13681.
- (84) Wang, H.; Wang, Y.; Ye, X.; Hayama, H.; Sugino, H.; Nakano, H.; Nakano, T. π -Stacked poly(vinyl ketone)s with accumulated push-pull triphenylamine moieties in the side chain. *Polym. Chem.* **2017**, *8* (4), 708–714.
- (85) Jeon, N. J.; Lee, H. G.; Kim, Y. C.; Seo, J.; Noh, J. H.; Lee, J.; Seok, S. I. o-Methoxy Substituents in Spiro-OMeTAD for Efficient Inorganic–Organic Hybrid Perovskite Solar Cells. *J. Am. Chem. Soc.* **2014**, *136* (22), 7837–7840.
- (86) Diaz, A. F.; Martinez, A.; Kanazawa, K. K.; Salmón, M. Electrochemistry of some substituted pyrroles. *J. Electroanal. Chem. Interfacial Electrochem.* **1981**, *130*, 181–187.
- (87) Seo, E. T.; Nelson, R. F.; Fritsch, J. M.; Marcoux, L. S.; Leedy, D. W.; Adams, R. N. Anodic Oxidation Pathways of Aromatic Amines. Electrochemical and Electron Paramagnetic Resonance Studies. *J. Am. Chem. Soc.* **1966**, *88* (15), 3498–3503.
- (88) Schramm, R. F.; Wayland, B. B. Oxidation of metallic palladium by nitrosyl tetrafluoroborate. *Chem. Commun.* **1968**, *15*, 898–899.
- (89) Zhao, A. X.; Chien, J. C. W. Palladium catalyzed ethylene-carbon monoxide alternating copolymerization. *J. Polym. Sci., Part A: Polym. Chem.* **1992**, *30* (13), 2735–2747.